Contents lists available at *Dergipark*

Journal of Scientific Reports-A

journal homepage: *https://dergipark.org.tr/tr/pub/jsr-a*

E-ISSN: 2687-6167 ***Number 55, December 2023***

RESEARCH ARTICLE

Receive Date: 03.10.2023 *Accepted Date: 11.12.2023*

Synthesis and characterization of b-site controlled la-based high entropy perovskite oxides

İlker Yıldız

Central Laboratory, Middle East Technical University (METU), Ankara, 06800, Turkey, ORCID: 0000-0001-5761-655X

Abstract

High entropy perovskite oxide materials are a highly promising class of materials with a wide range of potential applications. They offer a unique combination of perovskite oxides and high entropy oxides, making them suitable for various fields, particularly in electrochemical energy storage systems and hydrogen production. Given the growing demand for clean energy and efficient energy storage solutions, the development of high entropy materials holds great significance. In this study, a cost-effective and rapid fabrication method was employed to produce several single-phase high entropy perovskite oxides by altering the B-site cations. The results demonstrated that these high entropy perovskite oxides could be synthesized with the same crystal structure, despite having significantly different elemental compositions. These variations in elemental composition led to differences in lattice parameters, metal-oxygen bond strengths, and oxygen vacancy content within the materials. Understanding and manipulating these factors can have important implications for the design of high entropy materials for energy storage and other applications.

Keywords: XPS; SEM; XRD; entropy oxides; perovskite

1. Main text

High entropy oxides (HEOs) are a significant breakthrough in multicomponent alloy and oxide systems [1], [2], and [3]. High entropy materials consist of five or more elements in one side of the single crystal phase. This feature gives a unique combination of properties that are unattainable in single crystal phase with conventional solid solutions [3], [4]. For example, high entropy perovskite oxides (HEPOs) combine the characteristics of high entropy oxides, such as long-term crystal and electronic structure stability, and the advantages of perovskite oxides, i.e., adjustable physicochemical properties [5], [6], and [7]. HEPOs are an intriguing and rapidly developing category of materials that have attracted considerable interest within the scientific community in recent times. These compounds are notable for their distinct crystal structures and the novel mix of cations they contain within the perovskite

framework, resulting in remarkable properties and a diverse array of potential uses. HEPOs have emerged as a forefront area of research that sits at the intersection of materials science, chemistry, and condensed matter physics.

Perovskite oxides are typically represented by the formula ABO_3, where the A-site consists of rare earth, alkaline, or alkaline-earth cations with a 12-fold coordination to oxygen atoms, while the B-site comprises transition metal cations coordinated by 6 oxygen atoms [8], [9]. Lanthanum-based perovskite oxides have found widespread use in various applications and have demonstrated excellent performance in electrochemical systems [10], [11], [12], and [13]. Furthermore, there have been reports of high entropy oxides and high entropy perovskite oxides synthesized using various methods. For instance, Jiang et al. synthesized 13 high entropy perovskite oxides such as $Sr(Zn_{0.2}Sn_{0.2}Ti_{0.2}Hf_{0.2}Mn_{0.2})O_3$, $Ba(Zr_{0.2}Sn_{0.2}Ti_{0.2}Hf_{0.2}Ce_{0.2})O_3$, and their derivatives using a high-energy ball mill [14]. Bayraktar et al. produced $(FeMnCrCoZn)_3O_4$, a high entropy spinel oxide, through a simple co-precipitation method [15]. Similarly, Nguyen et al. synthesized $La(CrMnFeCoNi)O_3$ using a sol-gel method [6].

Various rapid synthesis techniques have been developed to reduce production time for high entropy perovskite oxides. For example, Wang et al. utilized the flash sintering method to synthesize $Sr(Ti_{0.2}Y_{0.2}Zr_{0.2}Sn_{0.2}Hf_{0.2})O_3$, which is a promising approach for rapid synthesis [16]. Wu et al. synthesized a range of high entropy oxides using rapid joule heating, applying high currents (20-25 A) directly to the powders [17]. Dong et al. also employed rapid joule heating to synthesize high entropy oxide nanoparticles [18]. These methods have the advantage of significantly reducing the time required for high entropy oxide production.

In this study, equimolar $La(FeCoCrMnZn)O_3$ and non-equimolar $La(Fe_xCo_yCrMnZn)O_3$ (where x and y alternate between 0.1 and 0.3) high entropy perovskite oxides (HEPOs) were successfully synthesized using a modified sol-gel pechini method. The results revealed that all of the synthesized HEPOs share the same crystal structure, and their electronic structure is consistent, with the exception of the oxygen content. However, the variation in the mole fractions of elements leads to lattice distortion and an imbalance in the electronic structure, ultimately resulting in the formation of oxygen vacancies.

1.1. Structure and Method

The HEPOs were synthesized via sol-gel pechini method. The stoichiometric amount of metal nitrates was mixed with deionized (DI) water and stirred continuously until obtain a homogenous solution. After obtaining the solution, gelation agents such as citric acid and acrylamide were added to solution with molar ration of 3:1. Then, the solution stirred and heated until formed a gel. Afterwards, the gel is dried overnight to remove the physically bonded NO_2, and H_2O. Then finally these powders calcinated at 900 °C to obtain a single-phase high entropy perovskite oxide with desired chemical formulas.

1.2. Characterization of High Entropy Perovskite Oxides

The crystal structure of the $La(Fe_{0.2}Co_{0.2}Cr_{0.2}Mn_{0.2}Zn_{0.2})O_3$ (HEPO), $La(Fe_{0.1}Co_{0.3}Cr_{0.2}Mn_{0.2}Zn_{0.2})O_3$ (HEPO-Fe1), and $La(Fe_{0.3}Co_{0.1}Cr_{0.2}Mn_{0.2}Zn_{0.2})O_3$ (HEPO-Fe3) were studied by powder X-ray diffraction (XRD, Rigaku) with Cu Ka radiation from 10-90°. The surface morphologies and elemental distribution of the samples were analyzed using Scanning Electron Microscopy (SEM). Additionally, the chemical composition of the HEPOs was determined through X-ray Photoelectron Spectroscopy (XPS), utilizing Al Kα radiation. To ensure accurate measurements, all the XPS peaks were calibrated with the standard C 1s spectrum at 284.6 eV.

2. Results

The XRD patterns of the synthesized HEPOs are depicted in Figure 1. In Figure 1a, one can observe the XRD patterns for all synthesized HEPOs. The diffraction peaks at 23.1°, 32.9°, 40.4°, and 47.1° correspond to the main peaks of the orthorhombic HEPO structure, representing the (110), (020), (022), and (220) planes, respectively. As

demonstrated in the Rietveld refinement results shown in Figure 1b, c, and d, the HEPOs exhibit a pure single orthorhombic crystal structure with very low χ^2 values.

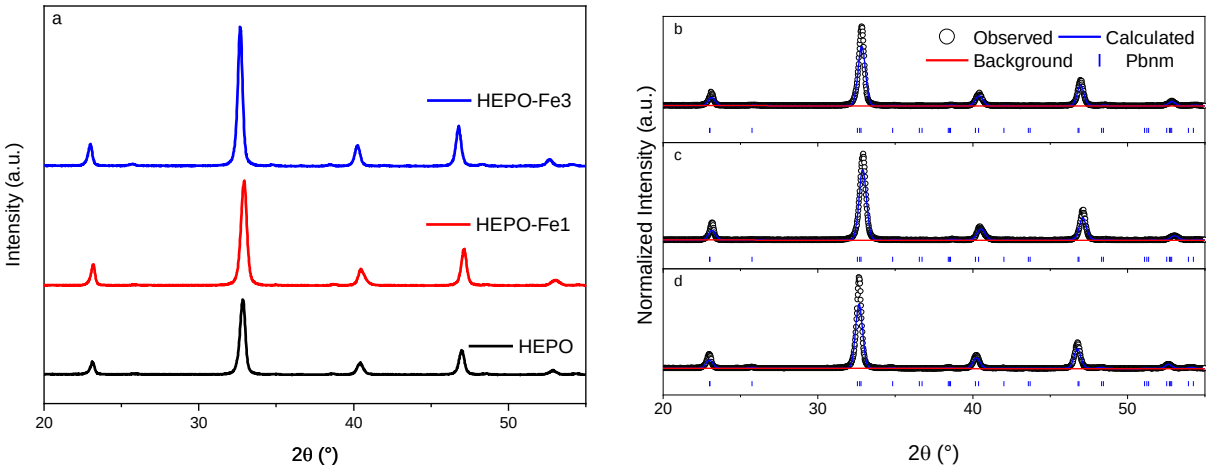

Fig. 1. (a) XRD patterns of the high-entropy perovskite series, (b)HEPO, (c)HEPO-Fe1, (d)HEPO-Fe3.

There are no additional peaks related to oxides or hydroxides of the elements, indicating the high purity of the synthesized HEPOs. Importantly, the type of crystal structure remains constant even when the B-site cation mole fractions vary. The primary effect of changes in the amount of elements is the alteration of the lattice parameters. This difference in lattice parameters is evident from the peak shift in the XRD pattern, as shown in Figure 1. The Rietveld refinement confirms that HEPOs possess an orthorhombic crystal structure with the Pbnm space group. The lattice parameters can be found in Table 1.

Table 1. Rietveld refinement analysis of HEPOs. Lattice Constants (*Å*).

Powder	**a**	**b**	**c**	**Volume (*Å*^{3})**	**Space Group**	**c2**
HEPO	5.53	5.49	7.78	236.248	Pbnm	1.49
HEPO-Fe1	5.51	5.47	7.77	234.400	Pbnm	1.71
HEPO-Fe3	5.53	5.51	7.79	237.093	Pbnm	2.39

The morphology and elemental distribution of the HEPOs were investigated through SEM and energy-dispersive X-ray spectroscopy (EDS) analysis. Figure 2 presents the SEM images of the HEPOs. It is evident that all the samples exhibit a similar shape and size, which underscores the precise control achieved during the synthesis process. The particle sizes fall within the range of 700-800 nm, and the particles display uneven and non-spherical morphologies.

The EDS mapping results, as shown in Figure 2, indicate that the elements are uniformly and homogeneously distributed throughout the particles and lattice. There is no elemental segregation observed for La, Fe, Co, Mn, Cr, Zn, and O. This implies that there are no oxide phases of the transition metals within the samples. Furthermore, this consistent distribution pattern is observed for all HEPOs, reinforcing the reliability and reproducibility of the synthesis method.

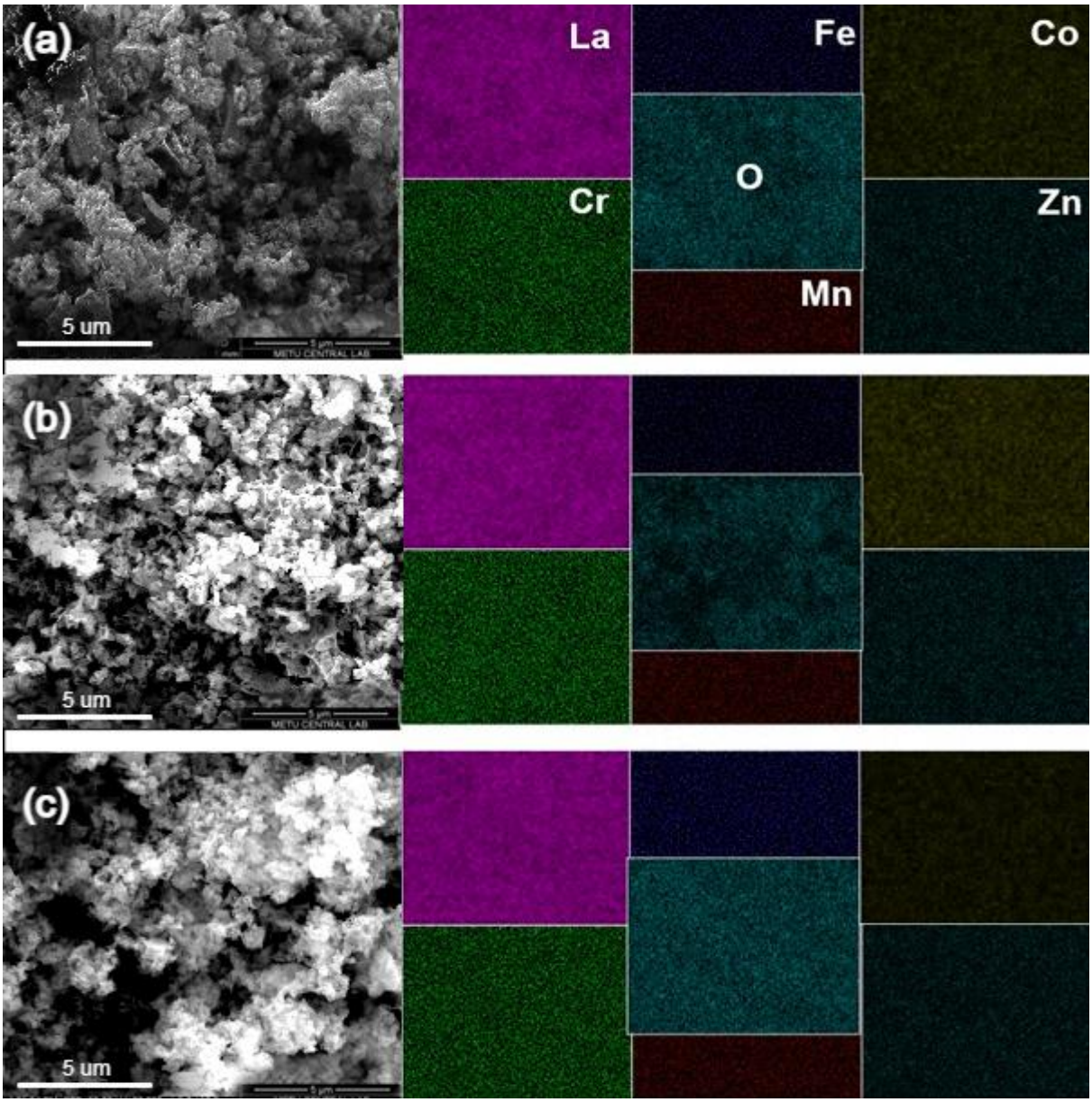

Fig. 2. SEM images and corresponding EDS mappings of (a) HEPO, (b) HEPO-Fe1, (c) HEPO-Fe3.

The XPS core level spectra of each element in the high entropy perovskite oxide structures are depicted in Figure 3. Every element's core level spectra were deconvoluted corresponding peaks. Figure 3 a, b, and c show the core level spectra of La for HEPO, HEPO-Fe1, and HEPO-Fe3, respectively. The La XPS spectra deconvoluted into four peaks corresponding to binding energies of 834.47 eV, 838.79 eV, 850.26 eV, and 855.58 eV. The spin-orbit splitting (SOS) observed in the La 3d5/2 and La 3d3/2 core-level XPS peaks is precisely measured at an energy differential of 16.8 eV. This energy separation, a characteristic feature of La core-level electron binding energies,

reflects the interaction between the spin angular momentum and orbital angular momentum of the electrons in the La atomic species under investigation [19].

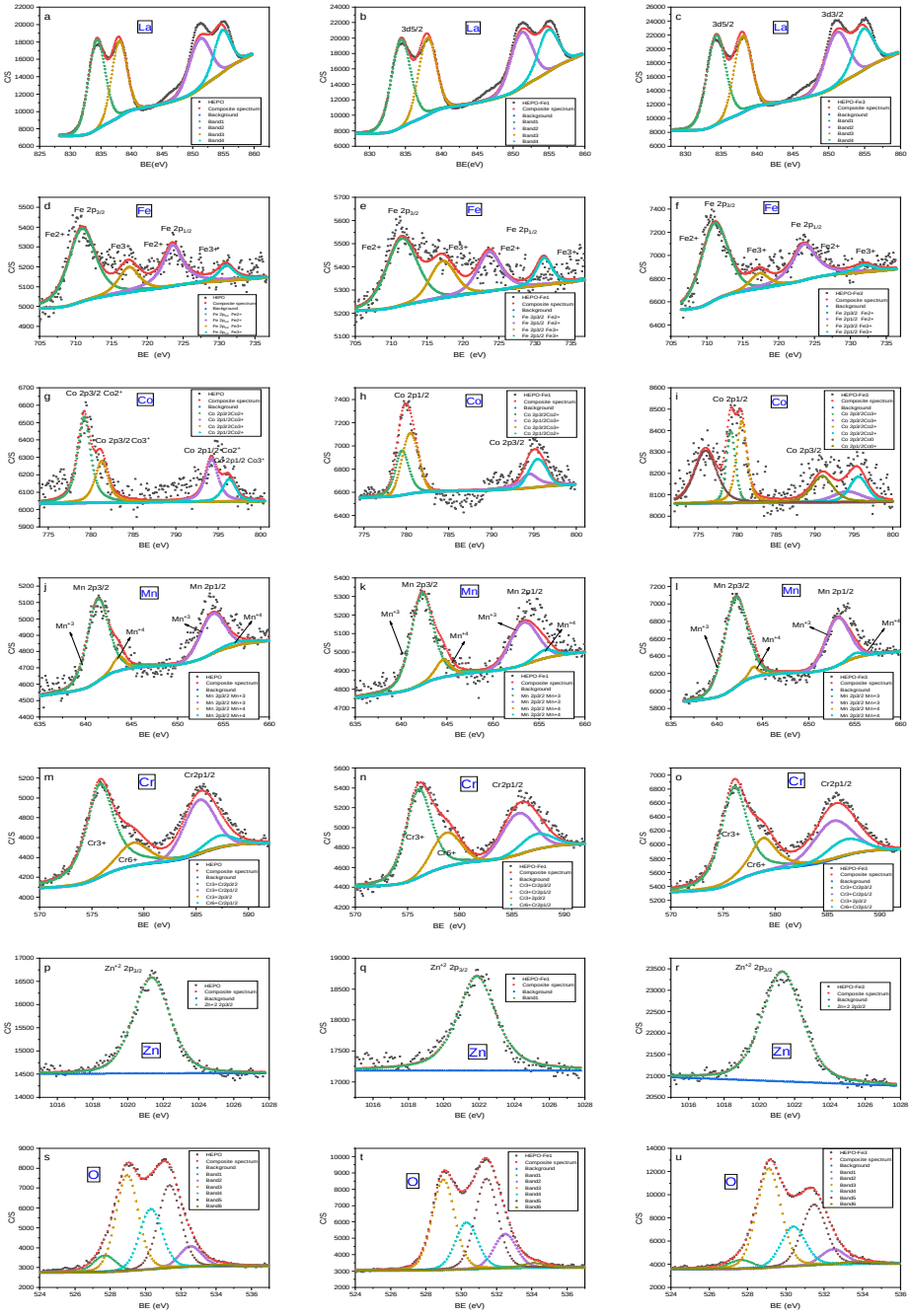

Fig. 3. XPS core level spectra of HEPO, HEPO-Fe1, HEPO-Fe3 for all elements, respectively.

Fe XPS core-level spectra are shown in Figure 3 d, e, and f for synthesized HEPOs. The Fe 2p core-level XPS spectrum exhibits a bifurcation into two spin-orbit doublets: Fe 2p3/2 and Fe 2p1/2, discernible at binding energies of 711.7 eV and 724.4 eV, respectively. Concurrently, the spectrum manifests shake-up satellite peaks at 719.1 and 736.2 eV. This complexity is further elucidated by the presence of two distinguishable peaks within each of the Fe 2p3/2 and Fe 2p1/2 components, indicative of two distinct chemical states of Fe, specifically Fe^{2+} and Fe^{3+} [20].

Consistent with existing literature, we have employed a fitting procedure for the Co 2p3/2 peaks, yielding binding energy values of 780.05 eV and 781.7 eV, which are attributed to Co^{3+} and Co^{2+} states, respectively. Similarly, for the Co 2p1/2 peaks, binding energy values of 795.73 and 797.32 eV correspond to Co^{3+} and Co^{2+} states, respectively. Additionally, weak satellite peaks at 786.9 eV and 805.08 eV are observed for HEPOs, as depicted in Figure 3g, h, and i. Notably, Co^{2+} is associated with the higher binding energy, aligning with prior XPS investigations of cobalt oxides [21], [22].

The Mn 2p spectra for HEPO, HEPO-Fe1, and HEPO-Fe3 are displayed in Figure j, k, l, respectively. The Mn XPS spectra are characterized by two discernible peaks situated at 642.7 and 654 eV, corresponding to the Mn 2p3/2 and Mn 2p1/2 spin orbits, respectively. Notably, additional features are observed within these spectral regions, with peaks at 642.3 and 653.7 eV associated with Mn^{3+} oxidation states, while peaks at 644.1 and 654.4 eV can be attributed to Mn^{4+} oxidation states [20].

The XPS spectra of the Cr2p core level, as illustrated in Figure 3m, n, and o, reveal the presence of two distinct sets of spin–orbit components centered at binding energies (BEs) of approximately 576.0 eV and 578.3 eV for the 2p3/2 state and 585.6 eV and 587.8 eV for the 2p1/2 state in all examined samples. This observation suggests the coexistence of two distinct chromium-based chemical species on the surface of the studied materials. The predominant component, characterized by the lower BE values of its two spin-orbit features, is attributed to Cr(III) species that are integrated within mixed transition metal spinel oxides, aligning with existing literature findings [23].

The XPS analysis of the O 1s spectra for HEPOs, as depicted in Figure 3s, t, u, can be resolved into four distinctive peaks. The initial peak corresponds to lattice oxygen species, typically associated with O^{2-}, situated at a binding energy of 529.6 eV. Following this, there is a peak attributed to highly oxidative oxygen species, typically represented by O_2^{2-} or O^-, positioned at 530.4 eV. Subsequently, there is a peak indicative of hydroxyl groups or surface-adsorbed oxygen, situated at a binding energy of 531.4 eV, typically corresponding to OH^- or O_2. Lastly, there is a peak associated with adsorbed molecular water or carbonates on the surface, appearing at 532.5 eV, which is typically representative of H_2O or CO_3^{2-} [24].

The core-level XPS spectra for Zn^{2+} in the 2p3/2 energy level typically exhibits a distinct peak as shown in Figure 3p, q, r. In XPS, the energy of emitted electrons is measured, and these energy levels correspond to the binding energy of 1022 eV. The XPS spectrum for Zn^{2+} 2p3/2 core-level electrons display a sharp and discernible peak at this binding energy. The precise shape and intensity of this peak can yield valuable information about the chemical state and local environment of the zinc atoms within the sample [25]. Measured binding energies are important in order to decide oxidation state of any characterized material also in the context of energy storage.

3. Conclusion

In conclusion, this study has underscored the immense promise of high entropy perovskite oxide materials as a versatile class of substances poised for extensive applications. With combining the distinctive characteristics of perovskite oxides and high entropy oxides, these materials exhibit remarkable potential in various domains, most notably in the realms of electrochemical energy storage systems and hydrogen production. Given the pressing global demand for environmentally sustainable energy solutions and efficient energy storage technologies, the advancement of high entropy materials assumes paramount importance. Within the scope of this investigation, we have successfully employed a cost-effective and expeditious fabrication method to synthesize a series of single-phase high entropy perovskite oxides by introducing alterations in the B-site cations. Our findings have elucidated that these high entropy perovskite oxides can be synthesized while maintaining consistent crystal structures, despite possessing

notably distinct elemental compositions. These variances in elemental makeup, however, have imparted consequential disparities in lattice parameters, metal-oxygen bond strengths, and oxygen vacancy levels within the materials. This newfound insight into the manipulation and comprehension of these crucial factors opens exciting avenues for the tailored design and optimization of high entropy materials for diverse applications, especially within the realm of energy storage. The potential ramifications of this research extend beyond the confines of our laboratory, offering an encouraging outlook for the development of next-generation materials that can drive sustainable energy technologies and bolster our collective pursuit of a greener future.

Acknowledgements

I would like to express my sincere gratitude to Assist. Prof. Dr. Çiğdem Toparlı for her valuable support throughout the research process. I also want to thank to Tuncay Erdil for his helpful feedback and support.

References

[1] E. P. George, D. Raabe, and R. O. Ritchie, "High-entropy alloys", *Nature Reviews Materials*, *4*(8), 515–534, 2019, https://doi.org/10.1038/s41578-019-0121-4
[2] M. V. Kante *et al.,* "A High-Entropy Oxide as High-Activity Electrocatalyst for Water Oxidation, *ACS", Nano*, *17*(6), 5329–5339, 2023, https://doi.org/10.1021/acsnano.2c08096
[3] C. M. Rost *et al.,* "Entropy-stabilized oxides", *Nature Communications*, *6*(1), 8485, 2015. https://doi.org/10.1038/ncomms9485
[4] F. Okejiri *et al.,* "Room- Temperature Synthesis of High- Entropy Perovskite Oxide Nanoparticle Catalysts through Ultrasonication- Based Method", *ChemSusChem*, *13*(1), 111–115, 2020, https://doi.org/10.1002/cssc.201902705
[5] Z. Liu *et al.,* "High-Entropy Perovskite Oxide: A New Opportunity for Developing Highly Active and Durable Air Electrode for Reversible Protonic Ceramic Electrochemical Cells", *Nano-Micro Letters*, *14*(1), 217, 2022 https://doi.org/10.1007/s40820-022-00967-6
[6] T. X. Nguyen, Y. Liao, C. Lin, Y. Su, & J. Ting, "Advanced High Entropy Perovskite Oxide Electrocatalyst for Oxygen Evolution Reaction", *Advanced Functional Materials*, *31*(27), 2101632, 2021, https://doi.org/10.1002/adfm.202101632
[7] L. Wang, M. D. Hossain, Y. Du, & S. A. Chambers, "Exploring the potential of high entropy perovskite oxides as catalysts for water oxidation", *Nano Today*, *47*, 101697, 2022, https://doi.org/10.1016/j.nantod.2022.101697
[8] X. Xu, Y. Zhong, & Z. Shao, "Double Perovskites in Catalysis, Electrocatalysis, and Photo(electro)catalysis", *Trends in Chemistry*, *1*(4), 410–424., 2019, https://doi.org/10.1016/j.trechm.2019.05.006
[9] W. J. Yin *et al.,* "Oxide perovskites, double perovskites and derivatives for electrocatalysis, photocatalysis, and photovoltaics", *Energy & Environmental Science*, *12*(2), 442–462, 2019, https://doi.org/10.1039/C8EE01574K
[10] J. Androulakis *et al.,* "LaSrMnCoO6: a new cubic double perovskite oxide", *Journal of Solid State Chemistry*, *173*(2), 350–354, 2023, https://doi.org/10.1016/S0022-4596(03)00109-9
[11] X. Cheng *et al.,* "Oxygen Evolution Reaction on $La_{1-x}Sr_xCoO_3$ Perovskites: A Combined Experimental and Theoretical Study of Their Structural, Electronic, and Electrochemical Properties", *Chemistry of Materials*, *27*(22), 7662–7672, 2015 https://doi.org/10.1021/acs.chemmater.5b03138
[12] T. Erdil *et al.,* "Facile Synthesis and Origin of Enhanced Electrochemical Oxygen Evolution Reaction Performance of 2H-Hexagonal $Ba_2CoMnO_{6-\delta}$ as a New Member in Double Perovskite Oxides", *ACS Omega*, *7*(48), 44147–44155, 2022, https://doi.org/10.1021/acsomega.2c05627
[13] J. T. Mefford *et al.,* "Water electrolysis on La1−xSrxCoO3−δ perovskite electrocatalysts", *Nature Communications*, *7*(1), 11053, 2016, https://doi.org/10.1038/ncomms11053
[14] S. Jiang *et al.,* "A new class of high-entropy perovskite oxides", *Scripta Materialia*, *142*, 116–120, 2018, https://doi.org/10.1016/j.scriptamat.2017.08.040

[15] D. O. Bayraktar, E. Lökçü, C. Ozgur, T. Erdil, & C. Toparli, "Effect of synthesis environment on the electrochemical properties of (FeMnCrCoZn)(3)O-4 high- entropy oxides for Li- ion batteries", *International Journal of Energy Research*, *46*(15), 22124–22133, 2022, https://doi.org/10.1002/er.8749
[16] K. Wang *et al.*, "Fabrication of high-entropy perovskite oxide by reactive flash sintering", *Ceramics International*, *46*(11), 18358–18361, 2020, https://doi.org/10.1016/j.ceramint.2020.04.060
[17] H. Wu *et al.*, "Rapid Joule-Heating Synthesis for Manufacturing High-Entropy Oxides as Efficient Electrocatalysts", *Nano Letters*, *22*(16), 6492–6500, 2022, https://doi.org/10.1021/acs.nanolett.2c01147
[18] Q. Dong *et al.*, "Rapid Synthesis of High- Entropy Oxide Microparticles", *Small*, 2104761, 2022, https://doi.org/10.1002/smll.202104761
[19] S. Mickevičius *et al.*, "Investigation of epitaxial LaNiO3−x thin films by high-energy XPS", *Journal of Alloys and Compounds*, *423*(1–2), 107–111, 2006, https://doi.org/10.1016/j.jallcom.2005.12.038
[20] X. L. Wang, E. M. Jin, G. Sahoo, & S. M. Jeong, "High-Entropy Metal Oxide (NiMnCrCoFe)3O4 Anode Materials with Controlled Morphology for High-Performance Lithium-Ion Batteries", *Batteries*, *9*(3), 147, 2023, https://doi.org/10.3390/batteries9030147
[21] C. Alex, S. Sarma, S. C. Peter, & N. S. John, "Competing Effect of Co^{3+} Reducibility and Oxygen-Deficient Defects Toward High Oxygen Evolution Activity in Co_3O_4 Systems in Alkaline Medium", *ACS Applied Energy Materials*, *3*(6), 5439–5447, 2020 https://doi.org/10.1021/acsaem.0c00297
[22] E. Lökçü, Ç. Toparli, & M. Anik, "Electrochemical Performance of $(MgCoNiZn)_{1-x}Li_xO$ High-Entropy Oxides in Lithium-Ion Batteries", *ACS Applied Materials & Interfaces*, *12*(21), 23860–23866, 2020, https://doi.org/10.1021/acsami.0c03562
[23] P. Gupta, R. Bhargava, R. Das, & P. Poddar, "Static and dynamic magnetic properties and effect of surface chemistry on the morphology and crystallinity of DyCrO3 nanoplatelets", *RSC Advances*, *3*(48), 26427, 2013, https://doi.org/10.1039/c3ra43088j
[24] M. Suthar, A. K. Srivastava, R. K. Joshi, & P. K. Roy, "Nanocrystalline cerium-doped Y-type barium hexaferrite; a useful catalyst for selective oxidation of styrene", *Journal of Materials Science: Materials in Electronics*, *31*(19), 16793–16805, 2020, https://doi.org/10.1007/s10854-020-04234-5
[25] A. Radoń, Ł. Hawełek, D. Łukowiec, J. Kubacki, & P. Włodarczyk,, "Dielectric and electromagnetic interference shielding properties of high entropy (Zn,Fe,Ni,Mg,Cd)Fe2O4 ferrite", *Scientific Reports*, *9*(1), 20078, 2019, https://doi.org/10.1038/s41598-019-56586-6